

Comparisons of various model fits to the Iron line profile in MCG-6-30-15

R. Misra

Inter-University Centre for Astronomy and Astrophysics, Pune, India

F. K. Sutaria

Inter-University Centre for Astronomy and Astrophysics, Pune, India

Received _____; accepted _____

ABSTRACT

The broad Iron line in MCG-6-30-15 is fitted to the Comptonization model where line broadening occurs due to Compton down-scattering in a highly ionized optically thick cloud. These results are compared to the disk line model where the broadening is due to Gravitational/Doppler effects in the vicinity of a black hole. We find that both models fit the data well and it is not possible to differentiate between them by fitting only the ASCA data. The best fit temperature and optical depth of the cloud are found to be $kT = 0.54$ keV and $\tau = 4.0$ from the Comptonization model. This model further suggests that while the temperature can be assumed to be constant, the optical depth varies during the observation period. We emphasize an earlier conclusion that simultaneous broad band data (3 – 50 keV) can rule out (or confirm) the Comptonization model.

Subject headings: accretion disks—black hole physics—galaxies:individual
(MCG-6-30-15)—galaxies:Seyfert—line:profile

1. Introduction

A long (≈ 4.5 days) observation by ASCA of the Seyfert 1 MCG-6-30-15 revealed that the Iron line profile in this source is broad with velocity width of $> 10^{10}$ cm sec $^{-1}$ (Tanaka et al. 1995). A more detailed analysis of the data by Iwasawa et al. (1996) showed that the profile is variable and the line width is maximum when the source intensity is minimum. Broad Iron lines have also been detected in other AGN by ASCA (e.g. Nandra et al. 1997). The most straight forward interpretation of this feature is the disk line model where the line is broadened due to the combined effects of Doppler and gravitational red-shift in the vicinity of a black hole (Fabian et al. 1989). From modeling the X-ray data, Iwasawa et al. (1996) showed that the disk producing this line has to have an inner radius $\approx 1.2r_s$ where $r_s = GM/c^2$ is the Schwarzschild radius. This would imply that the black hole is spinning close to its maximal value. If this interpretation is correct then this would be the first direct observation of the strong gravitational effects expected in the vicinity of a black hole. This would strongly constrain theoretical models since the inner disk region has to be cold in order to produce the Iron line while at the same time the hard X-ray producing region would also have to be located close to the inner edge of the disk. Reynolds & Begelman (1997) have argued that if some of the Iron line emission arises from the region inside the last stable orbit, the black hole need not be a rotating one.

Sulentic et al. (1998) showed there was a disagreement between the inclination angle derived by fitting the Iron line profile and that from HI and H α measurements. Several AGN for which a broad Iron line was detected have the peak centroid close to 6.4 keV (Nandra et al. 1997). It was pointed out by Sulentic, Marziani & Calvani (1998) that this is not expected if the disks are oriented in random directions. They propose that the Iron line profile is a sum of two independent Gaussian lines in order to explain the different correlation relationships of the red and blue side with the source intensity. They

also claimed that there is a blue wing in the Iron line emission which cannot be explained by the disk line model. These discrepancies and the importance of the implication of the disk line model warrant a study of alternate models to explain the phenomenon. Due to the profound implications of being able to ‘observe’ the immediate vicinity of a supermassive black hole, it is important to examine models for the broad Iron line that do not require strong gravity.

As an alternative to the disk line model, Czerny, Zbyszewska and Raine (1991) proposed that the line is intrinsically narrow and it gets broadened due to Compton down scattering of the photons as they pass through an optically thick cloud. This model is referred to here as the Comptonization model. Both, the Comptonization and the disk line models, predict a broad Iron line with an extended red wing. However, the detailed spectral shape of the line in the two models is different. In particular the disk line model predicts a double peaked line profile while the Comptonization model predicts a smooth feature. The observed line profile in MCG-6-30-15 can be fitted well by the disk line model (Iwasawa et al. 1996), but so far, no fits of this data have been made to the Comptonization model. Fitting the data to the Comptonization model would yield values for the optical depth and the temperature of the cloud – parameters that can be used to test the physical feasibility for the existence of such a cloud.

Fabian et al. (1995) rejected the Comptonization model by arguing that the surrounding Comptonizing cloud has to have a radius $R < 10^{14}$ cms in order that the cloud be highly ionized and does not produce strong absorption lines. For a $10^7 M_{\odot}$ black hole this would imply that the Iron line producing region is smaller than $50r_s$ and gravitational effects would be important. The lack of a blue wing in the best disk-line fit to the line profile, implies that the temperature of the cloud should be $kT < 0.2$ keV, which is in apparent conflict with the expected Compton temperature of the cloud. Further a break

in the continuum around 20 keV is expected for the Comptonization model which has not been observed. On the other hand, Misra & Kembhavi (1998) pointed out that for a smaller sized black hole, the intrinsic Iron line produced may not be significantly broadened by gravitational effects. They calculated the equilibrium temperature of the cloud to be around 0.2 keV provided an intense UV source is assumed to be present in this source. They showed that the present broad band data for this source is consistent with the Comptonization model. In these arguments the temperature of the cloud was constrained by the absence of a blue wing in the fitted spectrum for the disk line model. However, the unfolded spectrum depends on the model used to fit the data. In other words, the inferred shape of the Iron line profile depends on the model used to describe the fit. It is important to obtain better estimates for the temperature and optical depths of the cloud in order to verify the arguments presented by Fabian et al. (1995). In this paper, we directly fit the observed line profile to the Comptonization model and hence obtain more realistic values of the cloud parameters.

The Comptonizing model raises several questions regarding the stability, geometry and dynamics of such a cloud. The origin of such cloud(s) is unspecified but some arguments for their existence are presented by Guilbert & Rees (1988) and Kuncic, Blackman & Rees (1996). Optically thick obscuring clouds may be responsible for the intensity dip in MCG-6-30-15 (McKernan & Yaqoob 1998 ; Weaver & Yaqoob 1998).

The broad line may also be an artifact of simplistic modeling of the continuum. If the underlying continuum is complex and not a simple power-law, residuals caused by this fit may have been interpreted as a broad line. In order to test this hypothesis, we fit the data to a narrow line and a broken power-law as the continuum.

In the next section we briefly describe the observations and data analysis technique, In §3 the three models used for the fitting are described. In §4 the results of the data analysis

is presented. In §5 we discuss the implications of the results and summarize the paper in §6.

2. Observations

ASCA observed MCG-6-30-15 from 1994 July 23 to 27 (Tanaka, Inoue & Holt 1994) and the data has been analyzed in detail by Iwasawa et al. (1996). The SIS data which has been analysed in this paper, was obtained in Faint/1CCD mode. We used screened events files supplied by the HEASARC online service for this observation, where the Faint mode data was already converted into Bright (B) and Bright2 (B2) modes for analysis. In this paper, we analyze the 3 – 10 keV data since below 3 keV the spectrum is affected by the partially ionized gas (“the warm absorber”) surrounding the source. Following Iwasawa et al. (1996), the data set was divided into three epochs of which the epoch labeled “high” encompasses the highest intensity level of the source. The epoch labeled “low” encompasses the lowest intensity level of the source. The rest of the observation was grouped into a single data set labeled “medium”. Data from both the SIS chips (SIS 1 and 2) for the Bright and Bright2 modes were grouped and analyzed together. Only the relative normalization between these four sets of data was allowed to vary, but in all cases the variation was found to be less than 2%.

3. Brief description of Models

3.1. Disk Line model

The disk line model of Laor (1991) assumes that the emission arises from an accretion disk around a black hole and includes general relativistic effects. The inner radius of the accretion disk is r_i , where $r_i = 1.235r_s$ and $r_i = 6r_s$ ($r_s = GM/c^2$) correspond to the case of a maximally rotating black hole and a non-rotating one respectively. The model is

parameterized by r_i , the outer radius r_o , the emissivity index ξ , the rest frame line energy (fixed at 6.4 keV) and line intensity. The emissivity index (ξ) specifies the dependence of the emissivity with radius. The continuum is assumed to be a power-law characterized by two parameters – photon index Γ and a normalization factor. Thus the total number of free parameters used for the fitting is six.

3.2. Comptonization model

The physical geometry of this model is that the central engine consists of a hard X-ray source and a cold (UV producing) medium. The X-rays impinge upon the cold medium and produce a fluorescence Iron line and a reflected spectrum. However, unlike the disk line model, the Iron line is produced sufficiently away from the black hole and is intrinsically narrow and is broadened by the presence of an extended Comptonizing cloud. It is important to note that for self consistency both the intrinsic power-law and Iron line are Comptonized by the surrounding cloud. In principle, a reflected component which peaks around 50 keV should also be taken into account. Since the ASCA observations are restricted to photons with energy less than 10 keV we can neglect the reflected component here (Iwasawa et al. 1996).

The intrinsic spectrum is assumed to be a power-law with photon index Γ and a narrow Gaussian line with $\sigma = 0.05$ keV and centroid energy $E = 6.4$ keV. The source is assumed to be surrounded by a highly ionized cloud with optical depth $\tau = n\sigma_T R$ at a temperature kT . The output spectrum is calculated using the Kompane'ets equation. The Comptonization model has seven parameters – τ , kT , the intrinsic photon index Γ , the line energy (fixed at 6.4 keV), the intrinsic width of the line (fixed at 0.05 keV), the line intensity and a normalization factor. Thus the total number of free parameters used for the fitting is five.

3.3. Broken power-law model

The broken power-law is an empirical model used to test the hypothesis that the Iron line in this source is narrow and the artificial broadening observed is due to complexities in the underlying continuum. The Iron line is assumed to be a Gaussian with width $\sigma = 0.2$ keV and centroid at 6.4 keV. The continuum is fit by a broken power-law characterized by a high energy photon index Γ_1 , a low energy photon index Γ_2 , a break energy E_B and normalization. Thus the total number of free parameters used for the fitting is five.

4. Results

The medium intensity (MI) data were fitted to the disk line model of Laor (1991) for later comparison with the Comptonization model. The best fit parameters to the former model are shown in Table 1 and the unfolded data is plotted in Figure 1. As mentioned by Iwasawa et al. (1996) this model fits the data well with $\chi^2/(\text{dof}) = 1377/(1421)$ (Table 1, first row). The inner radius $r_i (= 2.9r_s)$ is constrained to be less than $3.7r_s$. However, since the line is broader during the low intensity phase, the inner radius is probably close to 1.235 which corresponds to a maximally rotating black hole. Setting $r_i = 1.235r_s$ and refitting the data gave $\Delta\chi^2 = 1.0$ (Table 1, second row).

The low (LI) and high intensity (HI) data sets were fitted to the disk line model after setting $r_i = 1.235$, $r_o = 16.4$ and inclination angle $\phi = 32^\circ$. These parameters are not expected to change during the observation period and freezing them constrains the rest of the parameters. Moreover the the number of free parameters become equal to those of the Comptonization model (see below) which enables a direct comparison. The HI data set is formally well fit by the model with $\chi^2/(\text{dof}) = 1235/(1424)$ (see Table 1). There seems to be evidence for an additional narrow component (Iwasawa et al. 1996 ; Sulentic, Marziani

& Calvani 1998). The emissivity index ($\xi = 2.0^{+0.7}_{-0.7}$) does not vary significantly from the MI state. Much of the spectral change can be attributed to the slight change in the power-law slope. The line shape during the LI level is different from that of the MI data (Table 1). The line is broader as indicated by the increase in the the emissivity index ($\xi = 3.3^{+0.3}_{-0.6}$), since an higher ξ implies that more photons are produced closer to the Black hole. The data is again well fit by the model with $\chi^2 / (\text{dof}) = 967 / (1424)$.

The Comptonization model also fits the MI data well with $\chi^2 / (\text{dof}) = 1396 / (1423)$ although with a higher χ^2 than the disk line model (Table 2). The temperature of the Comptonizing cloud is found to be $kT = 0.54^{+0.20}_{-0.19}$ keV. This is hotter than the temperature estimated by best fit line profile for the disk line model which was $kT < 0.2$ keV (Fabian et al. 1995, Misra & Kembhavi 1998). The reason for this discrepancy is that fitting the data to the Comptonization model reveals a blue wing (Figure 2). The inferred spectral shape i.e. the unfolded spectra depends upon the model used to fit the data. Thus the absence of a blue wing in the unfolded spectrum for the disk line model cannot be used as an estimation of the temperature of the cloud. The LI and HI data sets were fitted after setting $kT = 0.54$. The HI data is well fit by this model $\chi^2 / (\text{dof}) = 1225 / (1424)$ (see Table 2). The fit is similar to the disk line model and again there seems to be evidence for an additional narrow component (Figure 3). Compared to the MI fit the optical depth and line strength have increased while the power-law index (Γ) remain unchanged within the limits of error. Thus in terms of the Comptonization model, the photon index variation in the fit to the disk line model can be attributed to the change in degree of Comptonization of the intrinsic continuum. However, the limited statistics of the data set and the presence of an additional narrow line does not allow for any concrete statements to be made. The LI is well fit with a larger optical depth $\tau = 6.7$ with $\chi^2 / (\text{dof}) = 969 / (1424)$. The larger optical depth leads to a broader line for this set.

Table 1: Spectral parameters for the disk line model of Laor (1991) for the intensity selected data sets. The parameters are the power-law photon index (Γ), the emissivity index (ξ), the inner radius (r_i) in r_s , the outer radius (r_o) in r_s , the line Intensity (I_{line} in units of 10^{-4} photons/sec/cm² and the inclination angle ϕ in degrees. The line energy is fixed at 6.4 keV.

Data set	Γ	ξ	r_i	r_o	I_{line}	ϕ	$\chi^2/$ (dof)
Medium	$2.05^{+0.04}_{-0.03}$	$1.9^{+0.7}_{-0.6}$	$2.9^{+0.8}_{-1.7}$	$16.4^{+1.6}_{-1.0}$	$2.1^{+0.3}_{-0.3}$	$32^{+1.5}_{-2.0}$	1377/(1421)
Medium	$2.05^{+0.034}_{-0.03}$	$1.8^{+0.4}_{-0.2}$	1.235	16.4	$2.25^{+0.25}_{-0.3}$	32	1378/(1424)
High	$2.20^{+0.06}_{-0.06}$	$2.0^{+0.7}_{-0.7}$	1.235	16.4	$2.89^{+0.82}_{-0.66}$	32	1235/(1424)
Low	$2.03^{+0.19}_{-0.18}$	$3.26^{+0.31}_{-0.54}$	1.235	16.4	$2.96^{+0.98}_{-0.91}$	32	967/(1424)

Table 2: Spectral parameters for the Comptonization model for the intensity selected data sets. The parameters are the power-law photon index (Γ), the optical depth (τ), the temperature of the cloud (kT) in keV and the line Intensity (I_{line}) in units of 10^{-4} photons/sec/cm². The line energy is fixed at 6.4 keV and the intrinsic line width is assumed to be $\sigma = 0.05$ keV. The difference in χ^2 between the disk line (Table 1) and Comptonization model is tabulated in the last column.

Data set	Γ	τ	kT	I_{line}	$\chi^2/$ (dof)	$\Delta\chi^2$
Medium	$1.93^{+0.05}_{-0.015}$	$4.16^{+0.33}_{-0.49}$	$0.54^{+0.2}_{-0.19}$	$2.22^{+0.55}_{-0.36}$	1396/(1423)	+18
High	$1.96^{+0.12}_{-0.05}$	$5.32^{+0.62}_{-0.94}$	0.54	$3.71^{+1.07}_{-1.03}$	1225/(1424)	-10
Low	$1.76^{+0.18}_{-0.44}$	$6.69^{+2.37}_{-1.20}$	0.54	$3.81^{+2.84}_{-1.69}$	969/(1424)	+2

Since the data is from a narrow band (3 - 10 keV) both spectral slopes of the broken power-law model cannot be constrained. Therefore, the MI data is fit to the broken power-law model with the high energy photon index fixed at 2.0. This gives an unacceptable fit with $\chi^2 / (\text{dof}) = 1506 / (1424)$. An Acceptable fit was obtained when the high energy photon index was set to 2.5 with $\chi^2 / (\text{dof}) = 1422 / (1424)$. The HI and LI data sets can also be fitted by this model provided the high energy photon index is 2.5 (Table 3).

5. Discussion

The fit to the disk line model to the MI and LI data set is marginally better than for the Comptonization model. The reduced χ^2 for both the models are less than unity. The reason for this degeneracy is that the spectral shape of the best fit disk line model does not have a clear double peaked feature (Figure 1). Instead the red wing of the line gradually extends to ≈ 5 keV and such a feature can also be due Compton down-scattering of photons. Thus, the narrow band (3 - 10 keV) data used here cannot differentiate between these two models.

Although the HI data set is formally well fit by the models, there is evidence for an additional narrow Iron line (Iwasawa et al. 1996) in the residual plots. This could be due to a real additional narrow Iron line (Sulentic, Marziani & Calvani 1998) or because the Iron line shape is variable in a time scale shorter than the observation time ($\approx 10^5$ secs). In the latter scenario the observed shape of the Iron line would be the time-averaged profile and therefore could not be described by time-independent modeling.

Since there are no strong X-ray absorption features in this source the size of the Comptonizing cloud has to be smaller than $R < 10^{14}$ cms (Fabian et al. 1995). For a $10^6 M_\odot$ black hole this corresponds to about $\approx 300 r_s$. The intrinsic Iron line produced in

this case will not be significantly broadened by gravitational red-shift or Doppler effects. However if the black hole mass is larger, these effects would be important and the observed profile would be complex combination of Comptonization and gravitational effects. In this work for simplicity we have assumed that the intrinsic line is narrow ($\sigma = 0.05$ keV). The temperature of this cloud can be determined by equating the heating and cooling of the gas by Compton scattering. As described by Misra & Kembhavi (1998) the temperature of the gas depends upon the assumed UV flux of the intrinsic source. In Figure 4, the dashed line shows the assumed intrinsic spectrum for the source. The solid line is the output spectrum after the radiation passes through the cloud with optical depth $\tau = 4.0$ (the best fit value for the medium intensity data). The temperature of the cloud was calculated by balancing the input radiative power to the output power. The UV flux has been assumed here such that this temperature is equal to the best fit value $kT \approx 0.55$ keV. The UV luminosity is lower than that estimated by Misra & Kembhavi (1998) since the best fit value of the cloud temperature for the Comptonization model is 0.5 keV and not 0.2 keV as has been assumed earlier. The shape of the UV bump has been assumed here to have a black-body like shape. However, the equilibrium temperature is not sensitive to the spectral shape but rather to the total luminosity in the UV band compared to the X-ray band. The UV flux in MCG-6-30-15 is highly reddened and hence a UV bump is not directly observed for this source (Reynolds et al. 1997). Using the minimum value for the extinction, a lower limit of the intrinsic flux (F_{min}) has been calculated by Reynolds et al (1997) and is plotted in Figure 4 for comparison. The UV flux required by this model is about a factor ten larger than this minimum value. The reprocessed IR emission from covering dust in this source also indicate that the UV flux is much larger than F_{min} (Reynolds et al 1997).

The temperature of the gas will react to the changing intrinsic spectrum in a time scale

set by the time for the photons to diffuse out of the system,

$$t_c \approx \left(\frac{R}{c}\right)\tau^2 = 8 \times 10^4 \text{secs} \left(\frac{R}{10^{14} \text{cm}}\right) \left(\frac{\tau}{5}\right)^2 \quad (1)$$

The dynamical time scale is

$$t_d \approx \left(\frac{R}{v}\right) \approx 6 \times 10^4 \text{secs} \left(\frac{R}{10^{14} \text{cm}}\right)^{1/2} \left(\frac{M}{10^6 M_\odot}\right)^2 \quad (2)$$

where $v \approx (2GM/R)^{1/2}$ is the average bulk velocity of the plasma. Since this two time-scales are comparable to the observation time scale, the temperature and the optical depth can vary during the observations. The data is compatible with no change in temperature during the observation period with the change in the line profile being attributed to changes in the optical depth of the cloud (Table 2).

The continuum spectrum for energies ($E > 20$ keV) is greatly affected by the presence of a Comptonizing medium. For $E > 100$ keV the decrease in flux is nearly half of what is expected from a simple power-law model (Figure 4). The averaged Seyfert 1 spectrum from OSSE has been presented by Gondek et al. (1996). They find that at $E = 100$ keV, there is no significant decrease in the flux from the extrapolated power-law value. However, the statistics is not good enough to rule out a 50% decrease in flux. Moreover, the averaged spectrum may not represent the actual spectrum of MCG-6-30-15 at a given time. Significant differences in the continuum spectrum is also expected for $20 < E < 100$ keV. The analysis in this energy range is complicated by the presence of the reflection component which is significant only for $15 < E < 60$ keV. Nandra & Pounds (1994) analyzed the Ginga data for this source in $2 < E < 18$ keV range and find that a reflection component corresponding to a solid angle $\Omega_r \approx 2.0\pi$ is required to explain the data. Recently, Lee et al. (1998) analyzed the RXTE (PCA) data for this source for the energy band (2-20 keV). They find a reflection component corresponding to a larger solid angle $\Omega_r \approx 3.0\pi$. Preliminary analysis of the BeppoSax observation for this source (Matt 1998) requires a

$\Omega_r \approx 2.6\pi$. These results indicate that there is an excess flux at $E > 15$ keV which is in apparent contradiction to the Comptonization model. This excess can be explained within the framework of the Comptonization model if the intrinsic reflection component has a higher value of ≈ 1.5 times the fitted Ω_r (Misra & Kembhavi 1998). For $E \approx 50$ keV, the difference between the Comptonized power-law and power-law model is larger and can only be removed by invoking an extremely large unphysical solid angle for the reflected component $\Omega_r > 5\pi$. MCG-6-30-15 has been observed by the BeppoSax PDC instrument which is sensitive in the energy range ($13 < E < 200$ keV). Matt (1998) show the count spectrum for this source. However, the count flux at $E \approx 50$ keV is uncertain by about a factor of two. Hence it may not be possible to rule out the Comptonization model by this observation by BeppoSax. Similar longer duration broad-band ($3 < E < 100$ keV) coverage of this source is required to rule out or confirm the Comptonization model. Such an observation is also possible by HEXTE instrument in RXTE. An additional complication arises because the source (and hence the Comptonizing cloud) is known to be variable. Hence simultaneous observation in this range will be required.

Another explanation for these observations could be that the intrinsic line is narrow but the underlying continuum is complex i.e. not just a simple power-law. To test this hypothesis we have fit the data to a narrow line and a broken power-law. We find that the high energy spectral index has to be ≈ 2.5 for this model to fit the data. The recent BeppoSax data (Matt 1998) seems to contradict this result since the spectral index obtained was ≈ 2.0 . Moreover, it is also not clear which physical process will give a break energy $E_b \approx 5$ keV (Table 3).

6. Summary

The disk line model and the Comptonization model can fit the Iron profile of this source for the low and medium intensity data sets. The width and skewness of the Iron line profile can be reproduced if the source is surrounded by a cloud with optical thickness $\tau \approx 4$ and temperature $kT \approx 0.6$ keV. This temperature is higher than earlier estimates based on fits using the disk line model. The cloud will have this temperature provided there is a UV bump in the source which is not visible due to extinction.

The Iron line profile could also be narrow if the underlying continuum is complex. Modeling the continuum as a broken power-law allows for a reasonable fit only if the high energy photon spectral is ≈ 2.5 which may be in conflict with the recent BeppoSax observations.

As pointed out earlier by Misra & Kembhavi (1998), we emphasize the need for simultaneous long duration broad band (3 – 50 keV) observations of this source. Such observations will be able to rule out (or confirm) the Comptonization model and will strongly constrain any theoretical accretion disk models invoked to explain the AGN phenomena.

The authors would like to thank S. Raychoudhary and A. Kembhavi for useful discussions. This research has made use of data obtained from the High Energy Astrophysics Science Archive Research Center (HEASARC), provided by NASA’s Goddard Space Flight Center.

Table 3: Spectral parameters for the Broken power-law model for the intensity selected data sets. The parameters are the high energy power-law photon index (Γ_1), the low energy power-law photon index (Γ_2), the break energy (E_b) in keV and the line Intensity (I_{line} in units of 10^{-4} photons/sec/cm²). The line energy is fixed at 6.4 keV and the intrinsic line width is assumed to be $\sigma = 0.2$ keV. The difference in χ^2 between the disk line (Table 1) and the Broken power-law model is tabulated in the last column.

Data set	Γ_1	Γ_2	E_b	I_{line}	$\chi^2 / (\text{dof})$	$\Delta\chi^2$
Medium	2.5	$1.77^{+0.03}_{-0.03}$	$5.81^{+0.13}_{-0.15}$	$0.48^{+0.09}_{-0.08}$	1422/(1424)	+44
High	2.5	$1.91^{+0.05}_{-0.06}$	$5.28^{+0.27}_{-0.12}$	$0.96^{+0.16}_{-0.23}$	1208/(1424)	-27
Low	2.5	$1.45^{+0.10}_{-0.15}$	$5.30^{+0.29}_{-0.26}$	$0.27^{+0.19}_{-0.17}$	972/(1424)	+5

REFERENCES

- Czerny B., Zbyszewska M. & Raine, D.J. 1991, in Treves A., ed., Iron line Diagnostics in X-ray Sources, Springer-Verlag, Berlin, p 226.
- Fabian, A.C., Rees, M.J., Stella, L. & White, N.E. 1989, MNRAS, **238**, 729.
- Fabian, A.C. et al. 1995, MNRAS, **277**, L11.
- Gondek, D. et al. 1996, MNRAS, **282**, 646.
- Guilbert, P. W. & Rees, M.J., 1988, MNRAS, **292**, 664.
- Iwasawa, K. et al. 1996, MNRAS, **282**, 1038.
- Kuncic, E.G., Blackman, E. G. & Rees, M.J., 1996, MNRAS, **283**, 1322.
- Lee, J.C., Fabian, A.C., Reynolds, C.S., Iwasawa, K. & Brandt, W.N., 1998, MNRAS, *in press*
- Laor, A., 1991, ApJ, **376**, 90.
- Matt, G. 1998, in Proc. of the ‘High Energy Processes in accreting black holes’, J. Poutanen & R. Svensson (eds). (astro-ph: 9811053)
- McKernan, B. & Yaqoob, T., 1998, ApJ, **501**, L29.
- Misra, R. & Kembhavi, A.K., 1998, ApJ, **499**, 205.
- Nandra, K. & Pounds, K.A. 1994, MNRAS, **268**, 405.
- Nandra, K., George, I.M., Mushotzsky, R.F., Turner, T.J. & Yaqoob, T. 1997, ApJ, **477**, 602.
- Reynolds, C. S. & Begelman M. C. 1997, ApJ, **488**, 109.
- Reynolds et al., 1997, MNRAS, **291**, 403.
- Sulentic, J. et al., 1998, ApJ, **501** 54.

Sulentic, J., Marziani, P. & Calvani, M., 1998, ApJ, **497**, L65

Tanaka, Y., Inoue, H. & Holt, S.S., 1994, PASJ, **46**, L137

Tanaka, Y. et al., 1995, Nature, **375**, 659.

Weaver, K. A. & Yaqoob, T., 1998, ApJ, **502**, L139.

Fig. 1.— The unfolded spectra and best fit disk line model of Laor (1991). The medium intensity data from both chips (SIS0 and SIS1) for Bright (B) and Bright2 (B2) modes are shown separately. The dotted line is the power-law while the solid line is the sum of the power-law and Iron line profile. The parameters of the fit are given in Table 1.

Fig. 2.— The unfolded spectra and best fit Comptonization model. The medium intensity data from both chips for Bright (B) and Bright2 (B2) modes are shown separately. The dotted line is the Comptonized power-law while the solid line is the sum of the power-law and Iron line profile. The parameters of the fit are given in Table 2.

Fig. 3.— The unfolded spectra and best fit Comptonization model. The High intensity (I3) data from both chips for Bright (B) and Bright2 (B2) modes are shown separately. The dotted line is the Comptonized power-law while the solid line is the sum of the power-law and Iron line profile. The parameters of the fit are given in Table 2.

Fig. 4.— The Comptonized multi-wavelength spectrum for MCG-6-30-15. The dotted line is the assumed intrinsic spectrum of the source while the solid line is the Comptonized one. The intrinsic component consists of a UV bump, a X-ray power-law and a reflection component. The flux of the UV bump is chosen such that the equilibrium temperature of the surrounding cloud is $kT = 0.55$ keV. Also shown is the estimated UV lower limit for this source (Reynolds et al. 1997). Maximum deviation occurs for $E > 50$ keV.

Figure 1

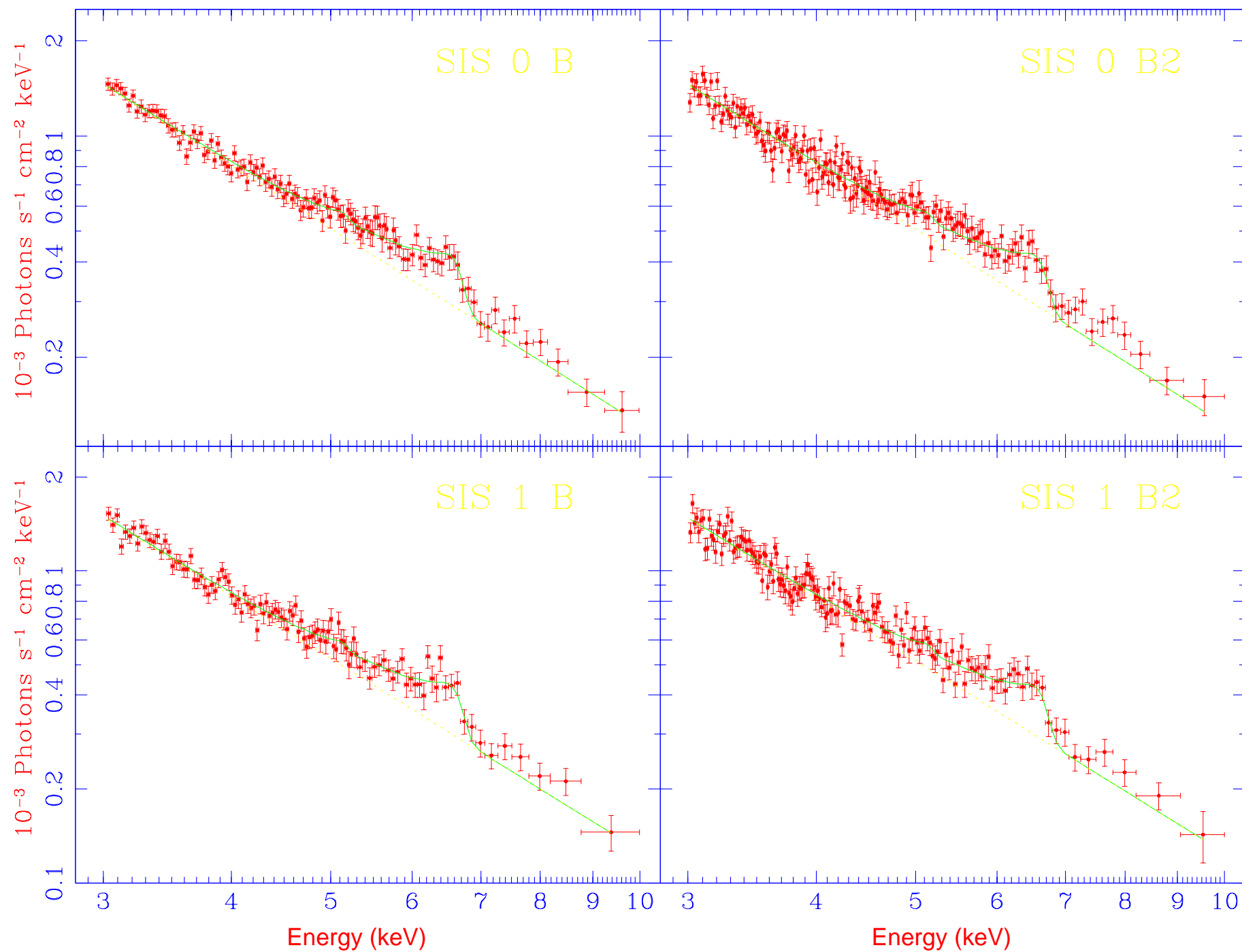


Figure 2

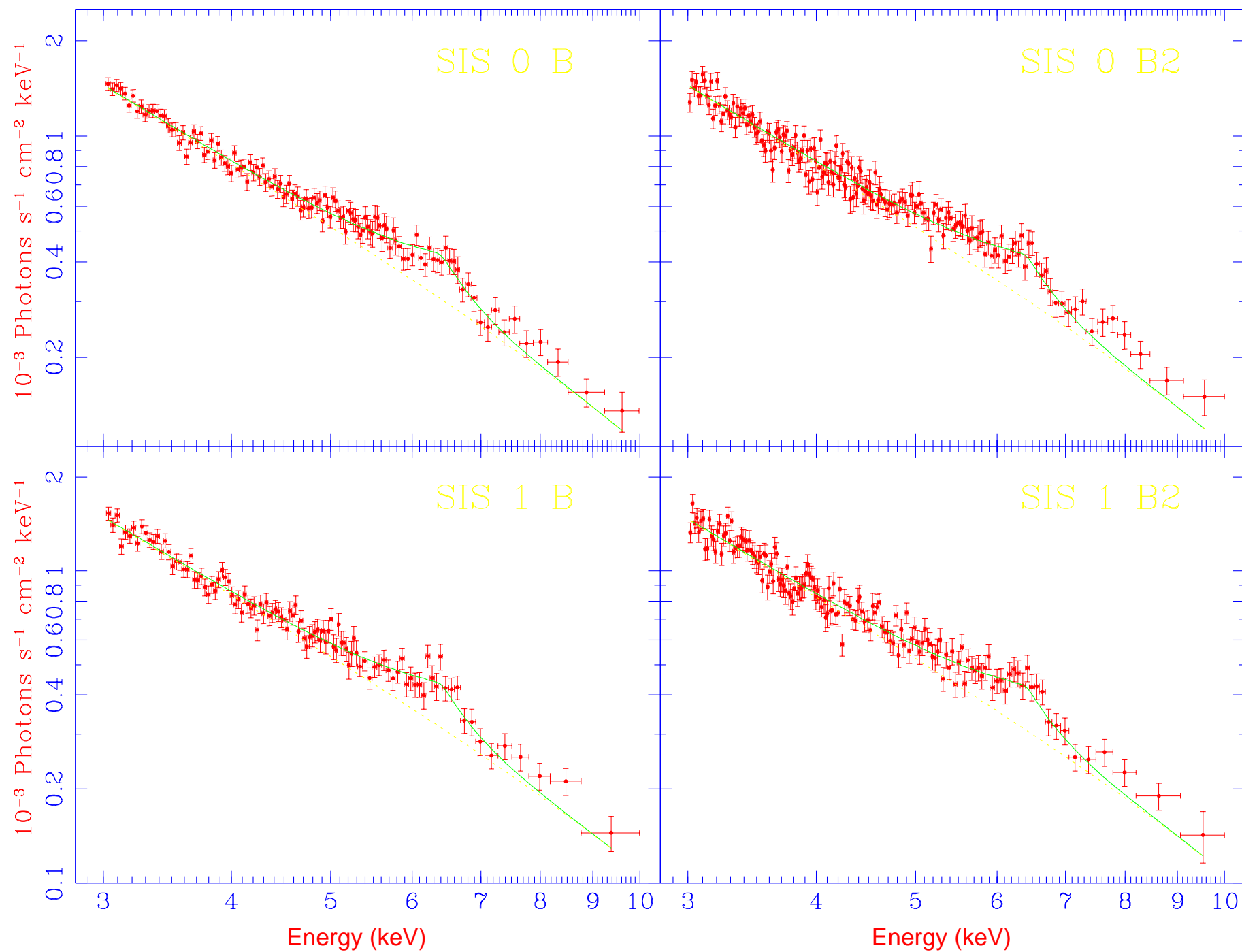


Figure 3

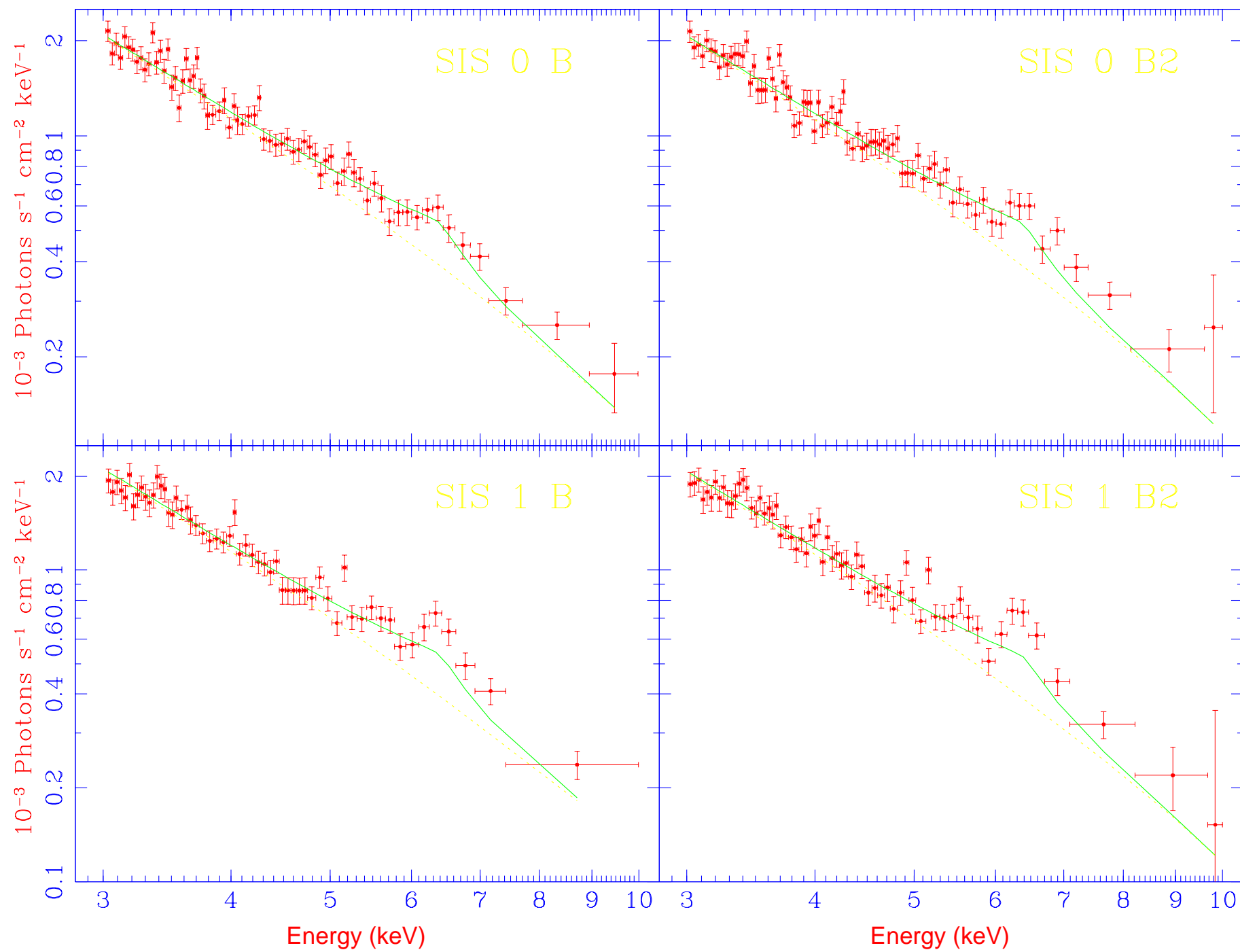


Figure 4

